INVESTIGATION OF PHASE COMPOSITION, MICROSTRUCTURE AND THERMAL BEHAVIOR OF Sn-3.0Ag-0.5Cu SOLDER ALLOYS WITH NI ADDITION

Tereza MACHAJDÍKOVÁ, Roman ČIČKA, Ivona ČERNIČKOVÁ, Libor ĎURIŠKA, Marián DRIENOVSKÝ

STU–Slovak University of Technology, Faculty of Materials Science and Technology, Trnava, Slovakia, EU

https://doi.org/10.37904/metal.2024.4900

Abstract

The aim of this work is to analyze the phase composition, microstructure, and thermal behavior of Sn-3.0Ag-0.5Cu solders with (0.1, 0.4, 1, 4) wt% Ni addition using experimental techniques (scanning electron microscopy, energy-dispersive X-ray spectroscopy, X-ray diffraction, differential scanning calorimetry) and computational thermodynamics (Thermo-Calc). The results show that the microstructure of all samples consisted of β-Sn dendrites in eutectic matrix (β-Sn + Ag_3Sn) and elongated particles of Cu_6Sn_5 intermetallic phase. Ni is dissolved in Cu_6Sn_5 phase, and with an increasing amount of Ni, the Ni_3Sn_4 phase starts to form, at the expense of Cu_6Sn_5. With increasing Ni addition, the microstructure becomes coarser, mainly Cu_6Sn_5 and Ni_3Sn_4 phases with cracks observed mainly in the later phase. The low values of undercooling (3.6 ÷ 14.4) °C of samples were determined, compared to the reported value for SAC305 solder. The results show a very good agreement between experimental results – phase composition, eutectic temperature, enthalpy of phase transformation (eutectic transformation + melting of β-Sn dendrites) and results achieved using thermodynamic computations in Thermo-Calc software.

Keywords: Sn-Ag-Cu-Ni solders, microstructure, phase composition, thermal behavior, computational thermodynamics

1. INTRODUCTION

Solder alloys are a fundamental part of the electronics industry. Proper solder material and soldering methods ensure good integration of mechanical and electrical connections in the electronic devices. Lead-containing solders, tin-lead solders in particular, were the most popular type of solders in the past, mostly due to their good physical, mechanical, and metallurgical properties, as well as their low cost. However, the use of lead became restricted due to health and environmental concerns Environmental Protection Agency (EPA) [1]. This led to the adoption of lead-free alternatives, such as Sn-Ag-Cu (SAC) alloys have been proposed as the most promising lead-free solders for replacement of traditional Sn-Pb solder due to their good reliability, excellent creep resistance, and thermal fatigue characteristics [2]. However, challenges remain with SAC solders, including their composition and the formation of brittle compounds. Research has shown that small amounts of elements like nickel can enhance the properties of the solders, such as the microstructure and mechanical properties of SAC alloys [3-7]. Research primarily explores nickel additions from 0.03 wt% to 1 wt% in solder alloys, showing even 0.05 wt% nickel can improve microstructure [8-10], lead to lower undercooling [11], stabilize Cu_6Sn_5 in high-temperature hexagonal form [12] and suppress the formation and growth of Cu_3Sn at the Cu/solder interface [13], leading to higher tensile strength and creep properties of solders and solder joints [14]. This paper focuses on the effect of (0.1 – 4) wt% Ni addition on the microstructure and thermal behavior of Sn-3.0Ag-0.5Cu (SAC305) solder. The experimental results are then compared to the computational thermodynamics results and discussed.

2. MATERIALS AND METHODS

The Sn-3.0Ag-0.5Cu (SAC305) alloys with different additions of Ni (0.1, 0.4, 1, and 4 wt%), hereafter denoted as SAC305-01Ni, SAC305-04Ni, SAC305-1Ni, and SAC305-4Ni, were investigated using experimental techniques and computational thermodynamics. The four alloys were prepared from raw materials Sn, Ag, Cu, and Ni (of 99.95% purity). They were mixed in proper fractions; the overall mass of the mixtures was 50 grams. Then the mixtures were melted in an induction furnace under an argon atmosphere. For the microstructural analysis, metallographic preparation was carried out by standard procedures consisting of grinding (60#, 240#, 600#, 1200#, and 4000# SiC paper) and polishing by diamond suspension (9, 6, 3, and 1 μm). The microstructures of the solder alloys were analyzed by scanning electron microscopy (SEM) using JEOL JSM-7600F in backscattered electrons mode and the distribution of elements was analyzed by the energy dispersive X-ray spectroscopy (EDX) using Oxford Instruments X-max 50. X-ray diffraction analysis (XRD) was used to identify the phases present in the system. The XRD patterns were recorded in 2Theta in range (20÷90)° using PANalytical Empyrean instrument with PIXCel3D detector at 40 kV and 40 mA, using Co Kα radiation with step size of 0.026° and counting time 96 s per pixel per step. The XRD patterns were evaluated with the HighScore software. The following ICSD cards were used: 98-010-6071 (β-Sn), 98-000-2721 (Ag_3Sn), 98-010-6530 (Cu_6Sn_5), 98-010-5363 (Ni_3Sn_4). Differential scanning calorimetry (DSC) analysis was carried out to examine the melting and solidification behavior of the samples. Pyris Diamond DSC (PerkinElmer) was used for the measurements in nitrogen (purity 5.0) protective atmosphere. Four samples with a mass of about 50 mg were cut from the bulk specimens and sealed in an aluminum pan for DSC analysis. Two measuring cycles in the temperature range (30÷250) °C for each sample were carried out, with a heating rate of 10 K/min and cooling rate of 12 K/min. Computational thermodynamics was used to predict the phase equilibria in the system and to evaluate the melting behavior of the solders. Thermo-Calc software (version 2022a) and thermodynamic database of lead-free solder systems (TCSLD, version 4.1) were used for all calculations.

3. RESULTS

3.1 Phase analysis and microstructure of samples

The isopleth of the SAC305-xNi system calculated in Thermo-Calc is shown in **Figure 1**, showing that liquidus temperature steeply increases with an increasing amount of Ni up to above 700 °C for SAC305-4Ni. The red vertical lines in isopleth illustrate the compositions of the investigated samples. According to this the predicted phase composition of the samples at room temperature is: β-Sn, Cu_6Sn_5, Ag_3Sn, and from 1 wt% Ni the Ni_3Sn_4 phase appears. The predicted phase compositions of samples were verified by XRD analysis. These results confirmed the presence of β-Sn, Ag_3Sn, and small amounts of Cu_6Sn_5 in all samples. The Ni_3Sn_4 phase was found in sample SAC305-1Ni (in small amounts), and mainly in sample SAC305-4Ni containing the highest amount of Ni. The microstructures of samples are shown in **Figure 2**. The microstructure of the SAC305-01Ni sample consists of large primary grains of β-Sn surrounded by eutectic (β-Sn + Ag_3Sn) and elongated particles of Cu_6Sn_5 in the β-Sn matrix (**Figure 2a**). With the increasing amount of Ni (sample SAC305-04Ni) the microstructure becomes coarser, mainly the phase Cu_6Sn_5 (**Figure 2b**). The phase Ni_3Sn_4 appears in samples SAC305-1Ni (**Figure 2c**) and SAC305-4Ni (**Figure 2d**). Ni_3Sn_4 phase has also a coarse morphology in both samples, in sample SAC305-4Ni resembling the island-like structure containing some amounts of Cu_6Sn_5 phase. There were also many cracks in Ni_3Sn_4, not only near the interface with β-Sn but also in the bulk of this phase. The results from EDX analysis (**Figure 3**) show the distributions of Sn, Ag, Cu and Ni in the samples and fully confirm the identification of phases in the microstructure. In the case of samples containing a lower amount of Ni (SAC305-01Ni, SAC305-04Ni) nickel is dissolved only in Cu_6Sn_5 phase, while in samples containing higher amounts of Ni (SAC305-1Ni, SAC305-4Ni) most of the nickel is in the Ni_3Sn_4 phase and Cu_6Sn_5 phase is often formed in the vicinity of Ni_3Sn_4 phase and in this phase.

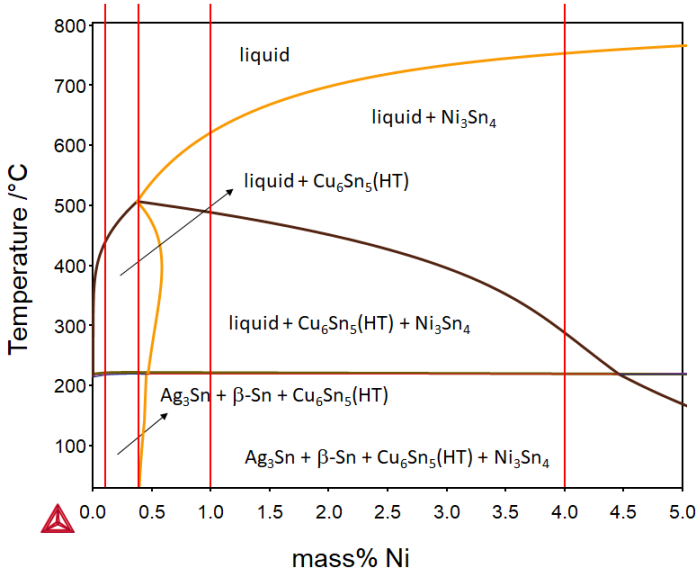

Figure 1 Calculated isopleth Sn-Cu of SAC305-Ni system, red vertical lines indicate the compositions of investigated samples (SAC305-01Ni, SAC305-04Ni, SAC305-1Ni, SAC305-4Ni)

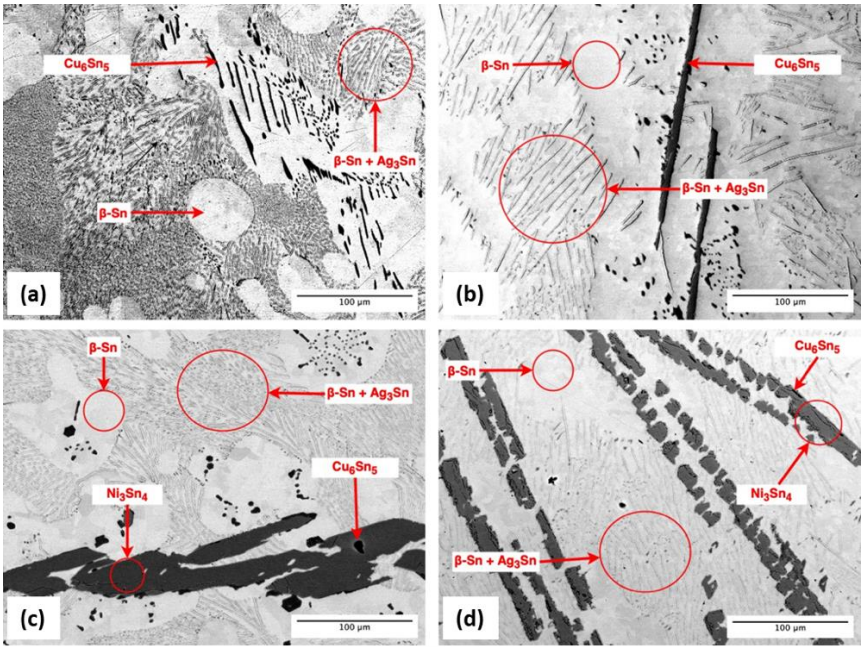

Figure 2 SEM microstructures of SAC305 with different addition of Ni: (a) 0.1 wt% Ni, (b) 0.4 wt% Ni, (c) 1 wt% Ni, and (d) 4 wt% Ni

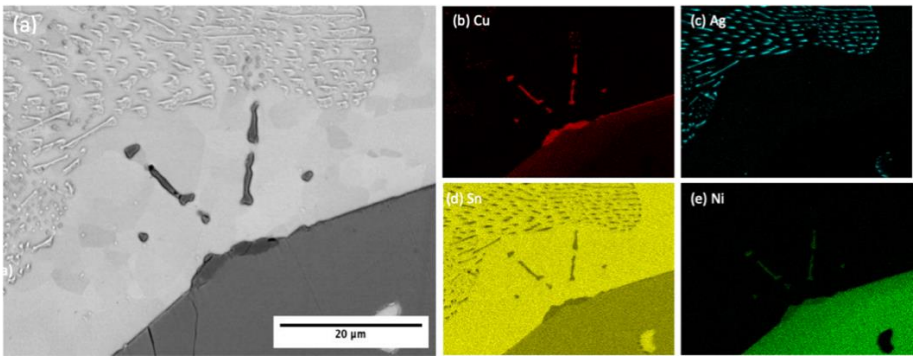

Figure 3 Microstructure of SAC305-1Ni sample (a) and corresponding distribution of elements (b-e) obtained using EDX

3.2 Melting and solidification behavior of solders

The DSC curves of all four samples are shown in **Figure 4** and they show that two thermal events during cooling of samples containing (0.1, 0.4, and 1) wt% Ni correspond to the formation of β-Sn phase and eutectic transformation, respectively. These two events are nearly overlapping in the case of sample SAC305-4Ni, as the temperature difference between these phase transformations is very small. The molar fractions of phases in SAC-xNi samples were calculated using Thermo-Calc and compared to DSC data (**Table 1**). It can be seen that the eutectic temperature of the samples determined using DSC is slightly lower for sample containing 0.1 wt% Ni (218.8 °C), for the samples containing (0.4, 1 and 4) wt% Ni the eutectic temperature is about 220 °C. The eutectic temperatures of the samples calculated using Thermo-Calc are in very good agreement with those experimentally determined using DSC, the relative differences are from 0.05% to 0.17%. Also, the calculated enthalpies of phase transformation (eutectic transformation + melting of β-Sn dendrites, i.e. the melting of the matrix of solder, as only IMCs Cu_6Sn_5 and $Ni_3Sn_4$are in solid state above this temperature) of the samples are in very good agreement with those experimentally determined using DSC, the relative differences are from 0.39% to 1.76%. It should be noted that the enthalpy of this phase transformation decreases with increasing amount of Ni, as the fraction of phases that do not participate in this phase transformation (Cu_6Sn_5, Ni_3Sn_4) is also increasing. **Table 1** also shows the values of undercooling of the samples. It can be seen that with the increasing amount of Ni the undercooling is also increasing, from 3.6 °C (sample SAC305-01Ni) to 14.4 °C (sample SAC305-4Ni).

Table 1 The experimental data of temperatures and enthalpies of phase transformation (eutectic transformation + β-Sn melting/solidification) during heating (T_{start}, T_{finish}, ΔH) and cooling (T^*_{start}, T^*_{finish}, ΔH^*). Undercooling ΔT is calculated as difference between T_{start} and T^*_{start}. The related Thermo-Calc data are denoted as (T_E, ΔH_{calc}).

Sample	Heating			Cooling			Undercooling	Thermo-Calc data	
	T_{start} (°C)	T_{finish} (°C)	ΔH (J/g)	T^*_{start} (°C)	T^*_{finish} (°C)	ΔH^* (J/g)	$\Delta T = T_{start} - T^*_{start}$ (°C)	T_E (°C)	ΔH_{calc} (J/g)
SAC-01Ni	218.8	226.1	64.46	215.2	208.3	64.26	3.6	218.70	63.59
SAC-04Ni	219.8	229.7	62.14	213.5	206.3	61.96	6.3	220.18	61.9
SAC-1Ni	219.8	229.1	60.98	213.0	206.4	60.84	6.8	220.15	60.49
SAC-4Ni	220.0	229.7	53.98	205.6	201.6	53.79	14.4	220.15	53.03

.

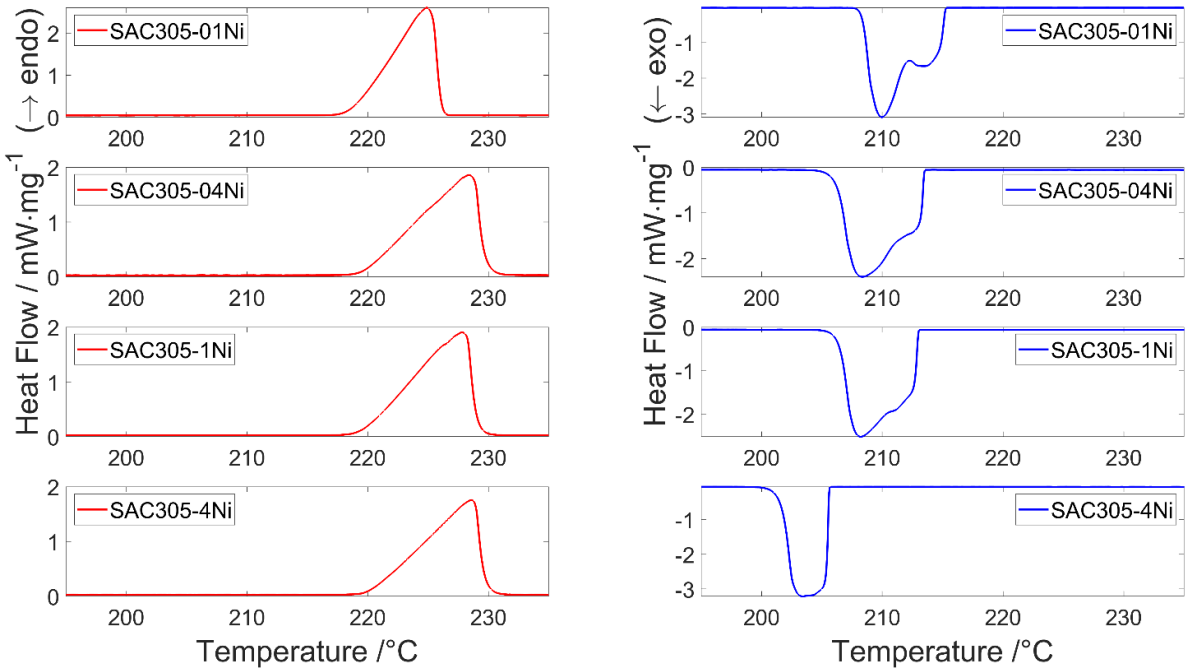

Figure 4 DSC curves of SAC305-xNi samples during heating (left) and during cooling (right), showing phase transformations (eutectic transformation + β-Sn melting/solidification)

4. CONCLUSION

In this work, the phase composition, microstructure, and thermal behavior of SAC305-xNi (x = 0.1, 0.4, 1, 4) solders were analyzed. The results are summarized as follows:

1) The microstructure of all samples consisted of β-Sn dendrites in eutectic matrix (β-Sn + Ag_3Sn) and elongated particles of Cu_6Sn_5 intermetallic phase. With the increasing addition of Ni, the coarsening of microstructure and an increasing amount of Cu_6Sn_5 was observed.
2) The eutectic temperature of all samples was (218.8 ÷ 220) °C. The Ni addition decreased the undercooling up to 3.6 °C (sample with 0.1 wt% Ni addition), compared to 24.2 °C reported for SAC305 solder [10]. But with increasing addition of Ni undercooling rises up to 14.4 °C (sample with 4 wt% Ni addition).
3) Ni substitutes Cu in Cu_6Sn_5 in the case of samples with a lower addition of Ni. When the Ni_3Sn_4 phase is formed in the samples with higher Ni addition, some amount of Ni is consumed during the formation of this phase and the rest of Ni is dissolved in Cu_6Sn_5.
4) The results show very good agreement between experimental results – phase composition, eutectic temperature, enthalpy of phase transformation (eutectic transformation + melting of β-Sn dendrites) with results achieved using thermodynamic computations in Thermo-Calc software.

ACKNOWLEDGEMENTS

This work was supported by the Slovak Grant Agency VEGA (project 1/0389/22), Young Researcher Grant at MTF STU (project 1332),and Slovak Research and Development Agency (project APVV-20-0124).

REFERENCES

[1] WU, C.M.L., YU, D.Q., LAW, C.M.T., WANG, L. Properties of lead-free solder alloys with rare earth element additions. *Materials Science and Engineering: R: Reports*. 2004. https://doi.org/10.1016/j.mser.2004.01.001.

[2] KOTADIA, H.R., HOWES, P.D., MANNAN, S.H. A review: On the development of low melting temperature Pb-free solders. *Microelectronics Reliability*. 2014. http://dx.doi.org/10.1016/j.microrel.2014.02.025.

[3] ZHU, T., ZHANG, Q., BAI, H., ZHAO, L., YAN, J. Improving tensile strength of SnAgCu/Cu solder joint through multielements alloying. *Materials Today Communications*. 2021. https://doi.org/10.1016/j.mtcomm.2021.10276.

[4] WANG, Y., WANG, G., SONG, K., ZHANG, K. Effect of Ni addition on the wettability and microstructure of Sn2.5Ag0.7Cu0.1RE solder alloy. *Materials & Design.* 2017. https://doi.org/10.1016/j.matdes.2017.01.046.

[5] KIM, K.S., HUH, S.H., SUGANUMA, K. Effects of fourth alloying additive on microstructures and tensile properties of Sn-Ag-Cu alloy and joints with Cu. *Microelectronics Reliability*. 2003. https://doi.org/10.1016/S0026-2714(02)00239-1.

[6] CHENG, H.K., HUANG, C.W., HSUAN, L., WANG, Y.L., LIU, T.F., CHEN, C.M. Interfacial reactions between Cu and SnAgCu solder doped with minor Ni. *Journal of Alloys and Compounds*. 2015. https://doi.org/10.1016/j.jallcom.2014.10.121.

[7] ZENG, G., McDONALD, S.D., GU, Q., TERADA, Y., UESUGI, K., YASUDA, H., NOGITA, K. The influence of Ni and Zn additions on microstructure and phase transformations in Sn-0.7Cu/Cu solder joints. *Acta Materialia*. 2015. https://doi.org/10.1016/j.actamat.2014.10.003.

[8] EL-DALY, A.A., EL-TAHER, A.M. Improved strength of Ni and Zn-doped Sn-2.0Ag-0.5Cu lead-free solder alloys under controlled processing parameters. *Materials & Design*. 2013. https://doi.org/10.1016/j.matdes.2012.12.081.

[9] EL-DALY, A.A., EL-TAHER, A.M., DALLOUL, T.R. Improved creep resistance and thermal behavior of Ni-doped Sn-3.0Ag0.5Cu lead-free solder. *Journal of Alloys and Compounds*. 2014. https://doi.org/10.1016/j.jallcom.2013.10.14.

[10] HAMMAD, A.E. Evolution of microstructure, thermal and creep properties of Ni-doped Sn-0.5Ag-0.7Cu low-Ag solder alloys for electronic applications. *Materials & Design*. 2013. https://doi.org/10.1016/j.matdes.2013.05.102.

[11] EL-DALY, A.A., EL-TAHER, A.M., DALLOUL, T.R. Enhanced ductility and mechanical strength of Ni-doped Sn-3.0Ag-0.5Cu lead-free solders. *Materials & Design*. 2014. https://doi.org/10.1016/j.matdes.2013.10.009.

[12] NOGITA, K., NISHIMURA, T. Nickel -stabilized hexagonal $(Cu,Ni)_6Sn_5$ in Sn-Cu-Ni lead-free solder alloys. *Scripta Materialia*. 2008. https://doi.org/10.1016/j.scriptamat.2008.03.002.

[13] YANG, Ch. SONG, F., LEE S.W. Impact of Ni concentration on the intermetallic compound formation and brittle fracture strength of Sn-Cu-Ni (SCN) lead-free solder joints. *Microelectronics Reliability*. 2014. https://doi.org/10.1016/j.microrel.2013.10.005.

[14] CHE, F.X., ZHU, W.H., POH, E.S.W., ZHANG, X.W., ZHANG, X.R. The study of mechanical properties of Sn-Ag-Cu lead-free solders with different Ag contents and Ni doping under different strain rates and temperatures. *Journal of Alloys and Compounds.* 2010. https://doi.org/10.1016/j.jallcom.2010.07.160.